Temperature-Pressure Phase Relationships in Niobium Pentoxide

J. L. Waring, R. S. Roth, and H. S. Parker

Institute for Materials Research, National Bureau of Standards, Washington, D.C. 20234

A pressure-temperature (P–T) section of the phase equilibrium diagram for Nb_2O_5 has been determined. Four single phase regions, H-Nb_2O_5, B-Nb_2O_5, and two L-Nb_2O_5 areas, were characterized by x-ray powder diffraction data. The superstructure of L-Nb_2O_5 was indexed on the basis of similarities to the known superstructures of L-Ta_2O_5 and confirmed with single crystal electron diffraction data. The correct unit cell is orthorhombic with $a = 6.168$, $b = 29.312$, $c = 3.938$ Å, with the b axis 8 times the subcell (8×3.664 Å).

Key words: Niobium pentoxide; phase relationships; pressure; temperature.

1. Introduction

Niobium pentoxide has been reported to occur in at least eight different polymorphic forms under varying experimental conditions. The polymorphs of Nb_2O_5 and their structural relationships to each other have been discussed by A. D. Wadsley and S. Andersson [1].[1] These authors postulated that some of the various modifications should have stability fields in the relevant ranges of the pressure-temperature (P–T) phase diagram. They put forward a "not impossible" phase diagram (fig. 1) based on no experimental evidence. S. Tamura [2] reported a temperature-pressure diagram (fig. 2) for Nb_2O_5 postulating the boundaries between H-Nb_2O_5 and L-Nb_2O_5 and B-Nb_2O_5 and L-Nb_2O_5 based on experiments utilizing an opposed piston apparatus. H-Nb_2O_5 is the stable polymorph which occurs at high temperatures and atmospheric pressure, L-Nb_2O_5 is the metastable polymorph formed during precipitation and B-Nb_2O_5 is the high pressure form [1]. In the present study only these three previously reported phases were found to occur in the system at the temperatures and pressures studied.

In this study, it was necessary to determine which of the multitude of possible polymorphs represent equilibrium phases and which represent metastable phases. The Nb_2O_5 specimens were equilibrated in an apparatus which is capable of heating materials in a uniform temperature zone up to about 1400 °C and 150,000 psi^2 isostatic pressure in an environment free of contaminants.
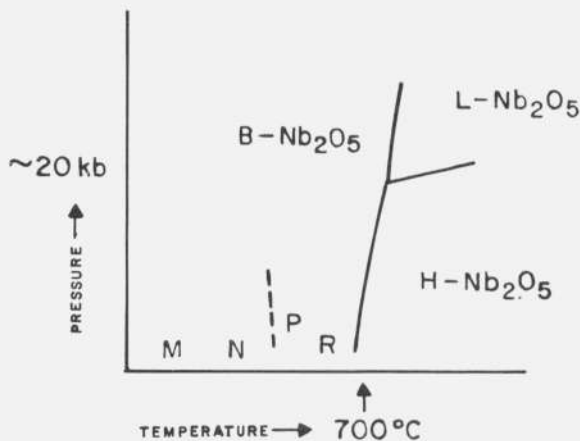

FIGURE 1. *Tentative temperature-pressure phase diagram for various Nb_2O_5 modifications (taken from Wadsley and Andersson [1] and modified according to present notation).*

2. Sample Preparation

The Nb_2O_5 used in this investigation was found by spectrographic analysis to contain less than about 0.01 percent Si, 0.001 percent Ca and Mg. The presence of As, Cu, and Ta was questionable. The starting materials were prepared as follows: The Nb_2O_5 (low temperature form) was dried at 130 °C for 19 h. Portions of the dried material were sealed in 5 mm O.D. × 25 mm long Pt tubes and heated to 1450 °C for 60 h to form H-Nb_2O_5, the high temperature polymorph. This material was reannealed in air at 1000 °C for 1 h to minimize any slight reduction which may have occurred. The B-polymorph of Nb_2O_5 was formed by heating the high temperature modification (H-Nb_2O_5)

---

[1] Figures in brackets indicate the literature references at the end of this paper.
[2] The use of psi, bar, and kbar follows the current common practice of workers in the field. Note that 1 bar $= 10^5$ N/m² (or pascal) $= 10^6$ dyn/cm² $= 0.9869$ atm $= 14.504$ psi. The accepted international standard (SI) unit of pressure is the pascal or newton per meter squared.
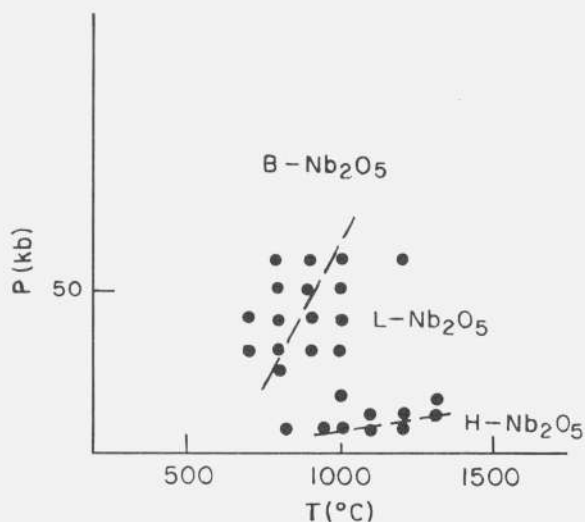
FIGURE 2. *Pressure/temperature/structure relationships for Nb_2O_5 (after Tamura [2]).*

FIGURE 3. *Schematic block diagram of pressure-temperature apparatus having a working range up to 1400 °C and 150,000 p.s.i.*

at 900 °C for 19 h at about 70,500 psi. For some experiments, $LiNbO_3$ or distilled H_2O was added to increase crystallinity and to determine if such impurities affect the equilibrium phase assemblage.

3. Apparatus

An internally heated pressure system similar to that described by Yoder [3] was used in this investigation. A block diagram of the apparatus is shown in figure 3. An air operated, two stage compressor (labeled A) supplies argon gas to the system at pressure to 30,000 psi. For higher initial pressures the valve (labeled B) is closed and the moving piston of an intensifier (labeled C) is advanced against the head of gas which has filled the vessel. The intensifier piston is advanced by hydraulic pressure supplied by an air driven oil compressor. The differential ratio of the intensifier is 5:1 thus providing a maximum pressure of 150,000 psi. The valve (labeled D) isolates the pressure vessel during a run. Pressures of up to 150,000 psi can be obtained in a few minutes *provided the system is tight.* Since a minimum of 16 h was needed to achieve equilibrium in most of the samples studied, at least in the lower $P-T$ range, particular attention had to be paid to obtaining a relatively leak free system. Experimental results were discarded if a pressure drop greater than 500 psi occurred during a run.

3.1. Pressure Measurement

The pressure was determined as a function of the change in resistance of a "seasoned" manganin wire coil when measured with a dc Carey-Foster Bridge [4]. The resistance of the manganin coils was approximately equal to $120\ \Omega$ and the coils were calibrated by the supplier against a dead weight gage. Two coils were used for a comparison measurement. One coil acted as a pressure sensor and the other served as a
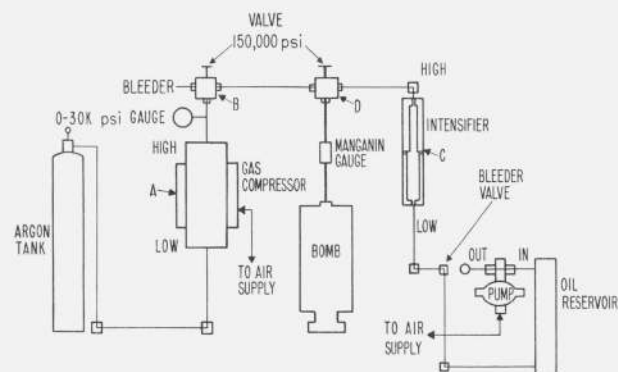
dummy gage for temperature compensation. A least squares fit by computer analysis of the correction data for the manganin coils used in this study has shown that the resistance-pressure curve in the range 0–150,000 psi can be described best by a parabolic equation of the type $R = B_0 + B_1P + B_2P^2$ where $B_0 = 1.20357$, $B_1 = 1.9926470 \times 10^{-5}$ and $B_2 = 8.0085893 \times 10^{-13}$. Errors in absolute pressure may be as much as 20 bar at 150,000 psi due to uncertainties in the pressure scale [3].

3.2 Temperature Measurement

The temperature was measured with a Pt-Pt10 percent Rh thermocouple. Bell [5] has shown that the effect of pressure on Pt-10 percent Rh thermocouples at the pressures attained in this work are within the limits of error in the temperature measurement. For this reason no correction for pressure has been applied to the temperature measurements. The temperatures reported can be considered accurate to at least ± 20 °C. Yoder [3] reported the results of probing the thermal gradient of his system with a thermocouple. A zone of even heating ± 5 °C was found to exist over a distance of about 5 cm. As our system is nearly identical, this time consuming process was not repeated.

4. Phase Equilibria

A $P-T$ phase equilibrium diagram for Nb_2O_5 (fig. 4) has been constructed from the x-ray data given in table 1. These data were obtained from specimens quenched (thermocouple indicates cooling to ambient temperature in less than a minute) by turning off the electrical power to the furnace and then reducing the pressure. Equilibrium was considered to have been approached when the x-ray powder diffraction patterns of specimens successively heated for longer times and/or at higher temperatures and/or pressures (quenched to ambient temperature and pressure) showed no significant change. X-ray diffraction powder patterns were made using a high angle record-
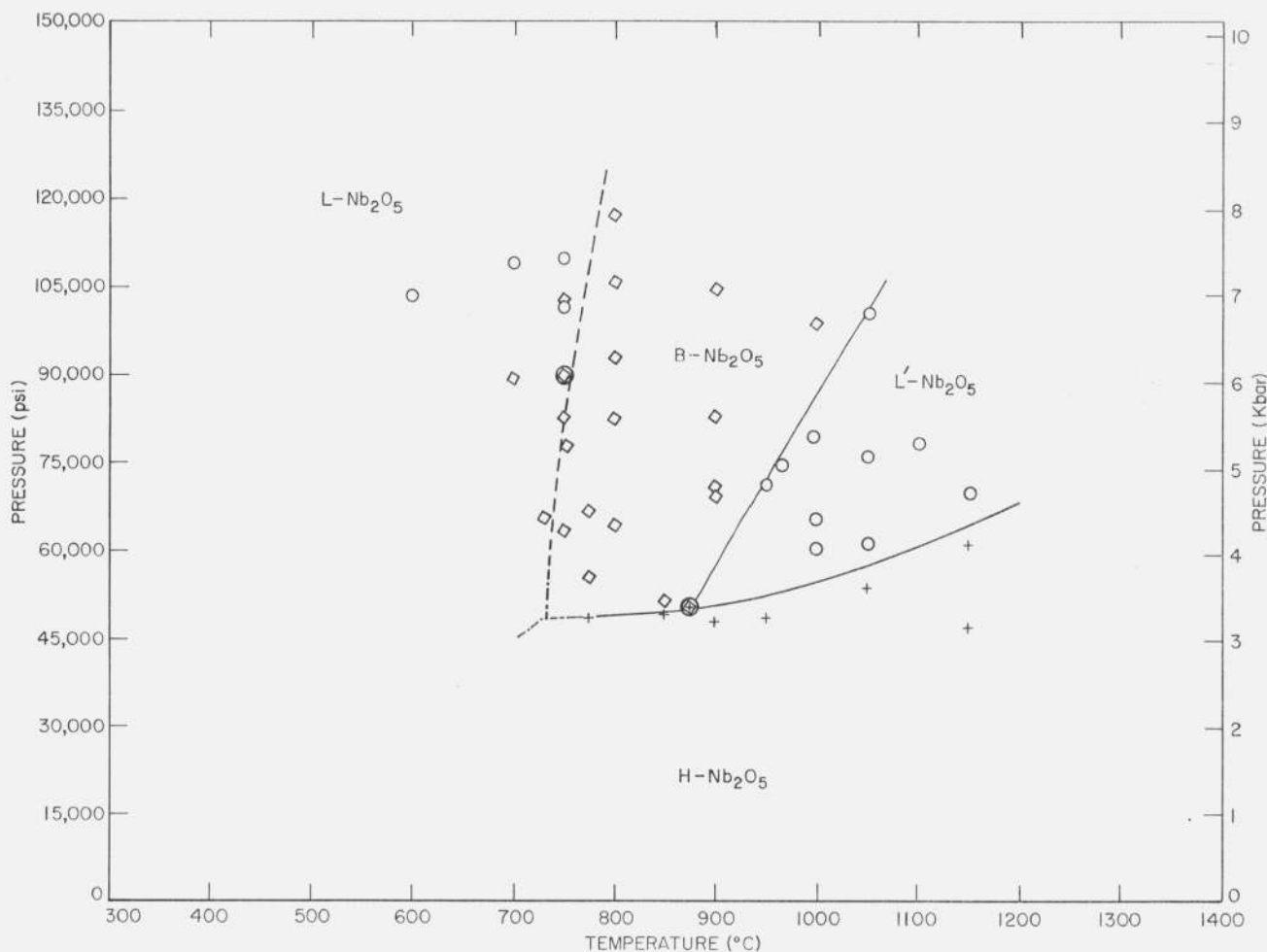
FIGURE 4. *Pressure-temperature* (P–T) *phase equilibrium diagram for* Nb_2O_5.

Dot dash curves — delineate phase boundaries which could not be determined. Dashed curve — delineates phase boundaries where reversibility was not established.

○ — L-Nb₂O₅
+ — H-Nb₂O₅
◇ — B-Nb₂O₅

Symbols refer to phases interpreted as equilibrium (see table 1 for experimental data).

ing Geiger counter diffractometer and nickel-filtered copper radiation with the Geiger counter scanning the 2θ angular range at $1/4°$ $2\theta/min$ and the radiation being recorded on the chart at $1°$ $2\theta/in$. The unit cell dimensions reported are estimated to be accurate within about two standard deviations.

The phase diagram can be described as consisting of four single phase regions in the temperature-pressure range investigated. They are designated $H-Nb_2O_5$, $L-Nb_2O_5$, $B-Nb_2O_5$ and $L'-Nb_2O_5$. In a previous study the N-form of Nb_2O_5 was synthesized at atmospheric pressure with the addition of $LiNbO_3$ [6]. However, in the present study this phase was found to transform to $B-Nb_2O_5$ at 800 °C and 64,000 psi and may be considered to become unstable with increasing pressure. No other polymorphs of Nb_2O_5 have been found to occur in this study.

4.1. H-Nb₂O₅ (High Temperature Form)

The crystal structure of the high temperature form of Nb_2O_5 ($H-Nb_2O_5$) was reported by Gatehouse and Wadsley [7]. The structure consists of infinite chains of 3×5 blocks of octahedra at one level and isolated blocks of 3×4 octahedra at the next level with tetrahedral positions at the block junctions. This phase, with a reported x-ray density of 4.55 [8], was found to occur at the highest temperature and lowest pressure (fig. 4). All experiments conducted in the $P-T$ range lower than that given in table 1 and figure 4 showed no change in the starting material. Therefore, the low temperature boundary of the $H-Nb_2O_5$ field could not be determined because equilibrium could not be achieved in this portion of the system in laboratory time.

707

Table 1. Temperature-Pressure Experimental Data for Nb_2O_5.

Heat Treatment[a][b]			X-ray Diffraction Analyses[c]
Temp °C	Time hr	Pressure psi	
600	144	103,000	H → H + L L → L + tr H
700	1	89,000	H → H + L L → L
700	168	108,500	H → L + tr H L → L
730	72	66, 200	B → B
746	22	101,100	H → L + H + tr B L → L + tr H and B
750	48	63,100	H → B L → B
750	96	77,200	H → L + H L → L + tr B
750	64	82,400	B → B
750	16	89,400	H → L + tr H L → L
750	127	107,200	B → B
751	168	108,000	H → L L → L
775	115	47,500	H → H L → L + tr H B → B + tr H
775	24	54,760	H → B + tr H L → B + L
775	43	66,540	H → B + tr L L → B + L
800	19	64,000	L → L + tr B
800	21	82,000	L → L + tr B
800	68	92,000	H → B + tr L L → B + L
800	24	105,000	H → B + L L → B + L
800	19	118,000	H → B + L L → L + H B → B
850	120	48,700	H → H L → L + H
850	144	51,400	H → B + tr H L → B + L
875	24	50,000	H → H L → B + L
900	112	47,500	L → L + tr H
900	19	68,000	H → B
900	16	70,400	H → B + H L → B + L
900	16	82,500	H → B + tr L L → B + L
900	36	104,000	H → B + tr L L → B + L
950	17	48,300	L → L + H
951	64	70,600	H → B + L L → L + tr B
965	64	75,000	H → L
995	65	79,160	H → L L → L
1000	19	60,000	L → L
1000	16	65,200	B → L
1000	48	98,000	H → L + B L → B + tr H
1050	16	53,000	H → B + L + tr H L → B + L
1050	192	60,750	H → H
1050	16	75,500	H → H
1050	16	100,000	H → L H → L
1100	16	77,700	H → L
1150	289	46,600	H → H L → L + tr H
1150	144	60,600	H → H L → H
1150	113	69,500	H → L L → L

Table 2. Indexed X-ray Diffraction Powder Pattern for $B\text{-}Nb_2O_5$ (CuKα radiation)[a]

hkℓ[b]	d_{obs}	$2\theta_{obs}$	$2\theta_{calc}$	I[c]
200	6.16	14.37	14.38	14
11$\bar{1}$	3.644	24.42	24.41	79
111	3.315	26.87	26.87	64
40$\bar{0}$	3.077	28.99	28.99	100
311	2.982	29.94	29.94	81
002	2.6868	33.32	33.33	43
31$\bar{1}$	2.5034	35.84	35.83	31
020	2.4422	36.77	36.77	11
40$\bar{2}$	2.3480	38.30	38.31	7
021 511 112	2.2218	40.57	40.54 40.55 40.59	14
510	2.1980	41.02	41.03	12
221	2.1667	41.65	41.65	7
600	2.0518	44.10	44.11	17
420	1.9133	47.48	47.49	29
51$\bar{1}$	1.8879	48.16	48.18	7
60$\bar{2}$	1.8827	48.30	48.30	7
022	1.8068	50.47	50.46	43
402	1.8057	50.50	50.52	36
11$\bar{3}$	1.7233	53.10	53.10	10
31$\bar{3}$	1.7081	53.61	53.59	21
71$\bar{1}$	1.7028	53.79	53.81	57
42$\bar{2}$	1.6920	54.16	54.14	29
130 11$\bar{3}$	1.6143	57.00	57.00 57.01	7
620	1.5710	58.72	58.73	6
13$\bar{1}$	1.5604	59.16	59.15	6
800	1.5382	60.10	60.09	13
80$\bar{2}$	1.5150	61.12	61.11	6
33$\bar{1}$	1.4947	62.04	62.05	9
62$\bar{2}$	1.4915	62.19	62.20	14
711	1.4831	62.58	62.60	26
602	1.4577	63.80	63.78	4
422	1.4512	64.10	64.10	7
313	1.4378	64.79	64.79	6
331	1.4217	65.62	65.62	14
71$\bar{3}$	1.3965	66.95	66.93	7
004	1.3433	69.98	69.99	4
820	1.3013	72.59	72.56	7
82$\bar{2}$ 60$\bar{4}$	1.2784	73.50	73.49 73.52	7

4.2. B-Nb₂O₅

The existence of $B\text{-}Nb_2O_5$ was first reported by Laves, Petter and Wulf [9] who described it as zeta-Nb_2O_5. Schäfer, Schulte, and Gruehn [10] formed several new phases from the reaction $Nb_2O_5(s) + 3NbX_5(g) \rightleftarrows 5NbOX_3(g)$ X = Cl, Br, or I. One of the new phases formed in this reaction was called B and is the same phase which Laves named zeta. In this paper, the B-nomenclature is used. The stability field of B is shown in figure 4. $B\text{-}Nb_2O_5$ is thus the medium temperature, high pressure polymorph of Nb_2O_5. $B\text{-}Nb_2O_5$ has not been previously synthesized by pressure equilibrium conditions below about 30 kbar [2], but was found to form under equilibrium conditions in the present work at pressures as low as 3.5 kbar.

This phase can be transformed reversibly, B-Nb$_2$O$_5$ ⇆ L-Nb$_2$O$_5$ and B-Nb$_2$O$_5$ ⇌ H-Nb$_2$O$_5$. However, B-Nb$_2$O$_5$ would not revert to L-Nb$_2$O$_5$ at the low temperature boundary (L'). This phase has been indexed after Laves, Petter, and Wulf [9] on the basis of a monoclinic unit cell. The parameters, $a = 12.744$, $b = 4.884$, $c = 5.563$ Å, and $\beta = 105°1.9'$, were refined by least squares analyses from the indexed x-ray powder pattern given in table 2.

4.3. L-Nb$_2$O$_5$ (Low Temperature Form)

a. Stability

The low temperature form of Nb$_2$O$_5$ (L-Nb$_2$O$_5$) was first reported by Brauer [11]. This is the apparently metastable form obtained when the material is precipitated from solution and crystallized at low temperatures. When heated this phase will gradually change to poorly formed H-Nb$_2$O$_5$. which becomes more crystalline with increasing time and temperature. Once H-Nb$_2$O$_5$ is formed it does not revert to L-Nb$_2$O$_5$ at atmospheric pressure at any temperature.

The only oxide known to stabilize L-Nb$_2$O$_5$ at a temperature in excess of 1000 °C at ambient pressure is Sb$_2$O$_4$ [12]. However, both F$^-$ and (OH)$^-$ probably also can be incorporated into this structure type [13, 14] which may also result in stabilization. Apparently L-Nb$_2$O$_5$ has a stability field at higher pressures and temperatures, as postulated by Wadsley and Andersson [1] and by Tamura [2]. In the present work, H-Nb$_2$O$_5$ was transformed to L-Nb$_2$O$_5$ and in turn L-Nb$_2$O$_5$ was transformed to H-Nb$_2$O$_5$ (see table 1). In figure 4, L-Nb$_2$O$_5$ is shown to occur as both the low temperature-high pressure and high temperature-high pressure (L'-Nb$_2$O$_5$) forms of Nb$_2$O$_5$ (see discussion sec. 5).

b. Structure

Numerous attempts to index the x-ray powder diffraction pattern of L-Nb$_2$O$_5$ have been reported in the literature. All such previous attempts were based on very limited powder data. Frevel and Rinn [15] first indexed L-Nb$_2$O$_5$ with a monoclinic unit cell and the orthorhombic subcell was indicated by Holser [16] to be similar to that of Ta$_2$O$_5$ and U$_3$O$_8$. An orthorhombic unit cell for L-Nb$_2$O$_5$ was proposed by Zvinchuck [17] with a b axis approximately 12 times the subcell. Terao [18] also showed an orthorhombic subcell and postulated a monoclinic supercell for L-Nb$_2$O$_5$ very similar to that of Frevel and Rinn [15]. From selected area electron diffraction of oxidized thin films, Spyridelis, Delavignette, and Amelinckx [19] reported that "in niobium pentoxide the spacing between the superlattice spots in the linear group is somewhat larger than in tantalum pentoxide corresponding to a smaller long spacing in direct space (which varies from 20 to 30 Å)". The authors stated that although the specimen temperature is difficult to estimate on beam heating they felt that sufficient specimen heating had occurred so that they were observing diffraction data taken from

a specimen of H-Nb$_2$O$_5$. Subsequently, precharacterized specimens of H-Nb$_2$O$_5$ were examined by Allpress. Sanders and Wadsley [20] by electron diffraction and found to be much different from the films described by Spyridelis et al. [19]. They concluded that, "in our opinion these films are much more likely to consist of low-temperature T-Nb$_2$O$_5$ (L-Nb$_2$O$_5$) or an oxygen-deficient phase, or a mixture of phases closely related to it."

With increased temperature and pressure L-Nb$_2$O$_5$ was found in the present work to become more crystalline and a number of superstructure lines become clearly evident in the x-ray diffraction pattern. This pattern is very similar to that of the phase 15Ta$_2$O$_5$ · 2WO$_3$, the smallest unit cell found for the L-Ta$_2$O$_5$ (L-Nb$_2$O$_5$) type phases [21, 22, 23]. The crystal structure of 15Ta$_2$O$_5$ · 2WO$_3$ has been reported by Stephenson and Roth [24] and the x-ray diffraction powder pattern was indexed on the basis of an orthorhombic unit cell with $a = 6.175$, $b = 29.29$, and $c = 3.874$ Å with the aid of intensities obtained from single crystal diffractometer data. For this composition, the b-axis is eight times the subcell ($b = 3.661 \times 8 = 29.29$ Å).

In the present work all of the lines of the powder pattern of L-Nb$_2$O$_5$ can be indexed on the basis of an orthorhombic cell with $a = 6.168 \pm .001$, $b = 29.312 \pm .001$ and $c = 3.936 \pm .001$ Å, with a and c similar to the values previously reported for the subcell. As is the case with 15Ta$_2$O$_5$ · 2WO$_3$, the b axis exhibits a multiplicity of 8 times the subcell and the true b axis is $b = 3.664 \times 8 = 29.312 \pm .001$ Å. The indexed x-ray diffraction powder pattern for L-Nb$_2$O$_5$ is given in table 3.[3]

Selected area electron diffraction patterns of L-Nb$_2$O$_5$ were made by J. G. Allpress, CSIRO, Melbourne, Australia, from a specimen heated to 1000 °C at 70,000 psi for 19 h. These patterns confirm that the correct unit cell is dimensionally orthorhombic with the parameters derived from the powder data. A typical example of diffraction from the $hk0$ plane is shown in figure 5. It can be seen in this diffraction pattern that there is a multiplicity of 8 along the b axis.

For a phase with $m = 8$ the ideal composition is M$_{16}$O$_{42}$ [21, 23, 24]. The compound 15Ta$_2$O$_5$ · 2WO$_3$ has the formula Ta$_{15}$WO$_{40.5}$ for eight subcells whereas the low temperature form of Nb$_2$O$_5$ would correspond to Nb$_{16}$O$_{40}$ with two oxygen ions missing and would have a slightly different ordering scheme. Since the crystal structure of 15Ta$_2$O$_5$ · 2WO$_3$ has been reported from single crystal data [24] it is possible to calculate the intensities of the x-ray diffraction powder pattern of this material. The Fortran program used for the computation was developed by Smith [25] and modified by Evans [26]. The calculated integrated intensities of the powder pattern agree quite well with those published for the observed powder data [22]. The integrated intensities for the L-Nb$_2$O$_5$ powder pattern were calculated utilizing the same coordinates. The

---

[3] R. Nolander and R. Norin (Acta Chem. Scand. **26** 3814 (1972)) have also indexed a powder pattern of "T-Nb$_2$O$_5$" with the unit cell: $a = 6.170$, $b = 29.25$, $c = 3.928$ Å.

Table 3. Indexed X-Ray Diffraction Powder Pattern for L-Nb$_2$O$_5$ (CuKα radiation)[a]

hkℓ[b]	d_{obs}	$2\theta_{obs}$	$2\theta_{calc}$	I_{obs}[c]	I_{calc}[d]
130	5.217	16.98	16.98	5	6
060	4.886	18.14	18.14	1	2
001	3.934	22.58	22.57	88	100
170	---	---	25.70	--	3
180	3.151	28.30	28.31	100	82
200	3.085	28.92	28.93	44	33
210	3.0680	29.08	29.09	15	22
190	---	---	31.03	--	<1
250	2.7298	32.78	32.78	5	1
260	2.6078	34.36	34.36	3	1
171	2.6080	34.46	34.46	1	2
181	2.4597	36.50	36.50	48	36
201	2.4278	37.00	37.00	21	14
211	2.4200	37.12	37.13	10	9
2,10,0	2.1250	42.51	42.51	3	1
1,13,0	2.1177	42.66	42.66	4	2
320	---	---	44.46	--	1
2,11,0	2.1534	44.91	44.92	6	1
330	2.0128	45.00	45.02	6	3
1,14,0	1.9828	45.72	45.72	1	2
002	1.9689	46.06	46.08	24	19
1,13,1	1.8646	48.80	48.79	6	2
370	---	---	49.34	--	2
0,16,0	1.8322	49.72	49.73	16	8
321	1.8084	50.42	50.41	1	1
380} 331}	1.7931	50.88	{50.88} {50.90}	23	12
390	---	---	52.60	--	1
371} 182}	1.6693	54.96	{54.96} {54.96}	24	20
0,16,1	1.6603	55.27	55.26	23	12
202	1.6592	55.32	55.32	23	12
2,15,0	1.6507	55.63	55.63	3	2
381	1.6316	56.34	56.34	15	9
391	---	---	57.94	--	1
2,16,0	1.5750	58.56	58.56	10	6
400	1.5420	59.94	59.93	4	1
410	1.5396	60.04	60.03	4	1
3,13,0	1.5195	60.92	60.93	3	<1
450	1.4912	62.20	62.19	1	<1
460	---	---	63.18	--	1
3,14,0	---	---	63.34	--	1
2,16,1	1.4622	63.58	63.57	9	5
401	1.4351	64.92	64.89	4	1
332	1.4070	66.38	66.39	3	1
372	---	---	69.80	--	1
0,16,2	1.3409	70.12	70.12	5	4
382	1.3255	71.06	71.06	8	6
003	---	71.90	---	--	2

[a] Specimen heated to 700°C at 108,500 psi for 168 hours in a sealed Pt tube and quenched.

[b] Indexed on the basis of an orthorhombic unit cell $\underline{a}$=6.199Å, $\underline{b}$=29.124Å, and $\underline{c}$=3.938Å.

[c] Observed intensity peak heights

[d] Calculated peak intensity using Fortran program described by D. Smith [25] and modified by E. Evans [26] (based on assumptions given in text).
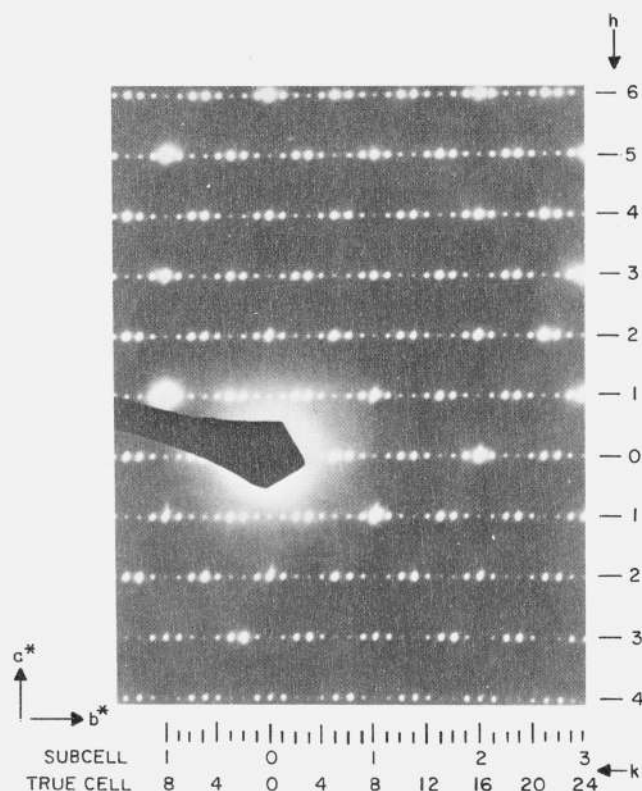

FIGURE 5. *Selected area electron diffraction photograph of the* hk0 *plane of a crystal of* L-Nb$_2$O$_5$ *taken from a specimen heated to 1000 °C at 70,000 psi for 19 hours.*

The superstructure of 8 times the subcell is clearly evident, as marked on the lower margin.

following assumptions were made for the calculation: space group Pm was chosen, and the z coordinates were fixed either at 0 or 1/2. Oxygen number 21 (notation of [24]) was found to be absent 3 out of 4 times in two unit cells of 15Ta$_2$O$_5 \cdot$2WO$_3$ and assumed to be completely absent in Nb$_2$O$_5$. The calculated peak intensities of L-Nb$_2$O$_5$ [25] (given in table 3) were found to be in good agreement with those observed in the x-ray powder diffraction pattern and to agree within experimental error with those calculated for 15Ta$_2$O$_5 \cdot$ 2WO$_3$. The L-Nb$_2$O$_5$ specimen from which these computations were made was heated at 700 °C for

168 h at 108,500 psi. Since crystals in this specimen were too small for single crystal x-ray diffraction studies, an attempt was made to grow single crystals of low Nb$_2$O$_5$ under pressure by the addition of H$_2$O. The resulting material was still very fine grained and unsuitable for single crystal x-ray diffraction studies. The x-ray powder pattern was indexed on the basis of a similar orthorhombic cell with the *b* axis multiplicity of 8 and slightly different unit cell dimensions, $a = 6.199$ Å, $b = 3.640 \times 8 = 29.124$ Å, and $c = 3.938$ Å.

5. Discussion

In figure 4 L-Nb$_2$O$_5$ and L'-Nb$_2$O$_5$ are shown to occur in two different portions of the system, separated by the field of B-Nb$_2$O$_5$. The x-ray diffraction patterns of specimens prepared in these two fields are identical except for degree of crystallinity. There are at least two possible interpretations of the data.

The first possibility is that an unknown high temperature phase may be postulated to cool metastably through the B-field and then transform to a stable phase of the L-Nb$_2$O$_5$ type. The low temperature form of Nb$_2$O$_5$ may possibly go through an infinite series of structurally subtle transitions of the sort reported for L-Ta$_2$O$_5$ [21, 24] involving a change in the multiplicity of the *b* axis. This type of transition would involve a

change in vacancy ordering and therefore in density. The structure of this original high temperature phase is, or course unknown, but may be postulated as being similar to H-Ta_2O_5 (previously found for Nb_2O_5 only from melted specimens containing some ZrO_2 [27]).

The second possibility is that a high temperature-high pressure polymorph may be assumed to be a phase of the L-Nb_2O_5 type which, on cooling through the B-field metastably, goes through a series of transitions to the $m=8$ phase at atmospheric temperature and pressure. In the first case L-Nb_2O_5 is the stable phase only in the low temperature-high pressure region. In the second case L-Nb_2O_5 is stable only in the high temperature-high pressure region and the B-polymorph is stable to ambient temperature at high pressures. Either case is equally possible even if the $m=8$ phase is maintained at all temperatures and pressures. The correct situation could only be solved by a high resolution high pressure-high temperature (above 900 °C) x-ray study. Unfortunately such an apparatus was not available.

---

6. References

[1] Wadsley, A. D., and Andersson, S., Perspectives in Structural Chemistry Vol. III, p. 1, edited by J. D. Dunitz and J. A. Ibers (John Wiley and Sons, New York, 1970).
[2] Tamura, S., J. Mater. Sci. 7 298 (1972).
[3] Yoder, H. S., Jr., Trans. Amer. Geophy. Union 31 827 (1950).
[4] Laus, F. A., Electrical Measurements, (McGraw-Hill, New York, 1938).
[5] Bell, P. M., Boyd, F. R., Jr., and England, J. L., Accurate Characterization of the High-Pressure Environment, Nat. Bur. Stand. (U.S.), Spec. Publ. 326, p. 63, edited by E. C. Lloyd (1971).
[6] Roth, R. S., Parker, H. S., Brower, W. S., and Waring, J. L., Fast Ion Transport in Solids, Solid State Batteries and Devices, sponsored by Advanced Study Institute, Belgirate, Italy (1972). Edited by W. vanGool (North Holland Publishing Co., Amsterdam, Holland, 1973), p. 217.
[7] Gatehouse, B. M., and Wadsley, A. D., Acta Cryst. 17 1545 (1964).
[8] Holzberg, F., Reisman, A., Berry, M., and Berkenbilt, M., J. Am. Chem. Soc. 81 3182 (1959).
[9] Laves, F., Petter, W., and Wulf, H., Naturwissenschaften 51 633 (1964).
[10] Schäfer, H., Schulte, F., and Gruehn, R., Angew. Chem. 76 536 (1964).
[11] Brauer, G., Z. anorg. allgem Chem. 248 1 (1941).
[12] Roth, R. S., and Waring, J. L., Amer. Min. 48 1348 (1963).
[13] Andersson, S., and Åström, Acta Chemica Scan. 18 2233 (1964).
[14] Jahnberg, L., and Andersson, S., Acta Chemica Scan. 21 615 (1967).
[15] Frevel, L. K., and Rinn, H. N., Anal. Chem. 27 1329 (1955).
[16] Holser, W. T., Acta Cryst. 9 196 (1956).
[17] Zvinchuck, R. A., Crystallography C.C.C.R. 3 744 (1958).
[18] Terao, N., Japanese Journal of Applied Physics 2 156 (1963).
[19] Spyridelis, J. S., Delavignette, P., and Amelinckx, S., Phys. stat. sol. 19 683 (1967).
[20] Allpress, J. G., Sanders, J. V., and Wadsley, A. D., Phys. stat. sol. 25 544 (1968).
[21] Roth, R. S., and Waring, J. L., J. Res. Nat. Bur. Stand. (U.S.), 74A (Phys. and Chem.), No. 4, 485–493 (July–Aug. 1970).
[22] Roth, R. S., Waring, J. L., and Parker, H. S., J. Solid State Chem. 2 445 (1970).
[23] Roth, R. S., and Stephenson, N. C., The Chemistry of Extended Defects in Non-Metallic Solids, p. 167, Edited by L. Eyring and M. O'Keeffe, (North Holland Publishing Co., Amsterdam, 1970).
[24] Stephenson, N. C., and Roth, R. S., Acta Cryst. B27 1110 (1971).
[25] Smith, D. K., A Revised Program for Calculating Powder Diffraction Patterns, Lawrence Radiation Laboratory, Livermore, Calif.
[26] Personal communication, E. Evans, National Bureau of Standards (1973).
[27] Roth, R. S., Waring, J. L., Brower, W. S., and Parker, H. S., NBS Special Publ. 364, p. 183, Proceedings of 5th Materials Research Symposium, Edited by R. S. Roth and S. J. Schneider (1972).

(Paper 77A6–793)